

STP 1611, 2018 / available online at www.astm.org / doi: 10.1520/STP161120170198

Rozbeh B. Moghaddam,¹ Daniel S. Belardo,¹ George Piscsalko,²
and Garland Likins²

1
2

Quality Control of Drilled Foundations for Base Cleanliness, Concrete Integrity, and Geometry

Citation

Moghaddam, R. B., Belardo, D. S., Piscsalko, G., and Likins, G., "Quality Control of Drilled Foundations for Base Cleanliness, Concrete Integrity, and Geometry," *10th International Conference on Stress Wave Theory and Testing Methods for Deep Foundations, ASTM STP1611*, P. Bullock, G. Verbeek, S. Paikowsky, and D. Tara, Eds., ASTM International, West Conshohocken, PA, 2018, pp. 223–237, <http://dx.doi.org/10.1520/STP161120170198>³

ABSTRACT

One of the important factors that influences the performance of drilled foundations is the construction method and procedure. To ensure proper construction, a quality control process is applied during and after drilled foundation installation. Considering the construction process for each type of drilled foundation, the evaluation of the drilled hole prior to concrete or grout placing and cage lowering has to be performed using the appropriate testing method. In the case of augered-cast piles, the bottom of the hole cleanliness or the cross-section area evaluation is performed using different tools from those used in the case of drilled shafts. The current state of practice includes several quality control inspection devices and non-destructive test methods for assessing the quality and integrity of drilled shafts as well as augered-cast piles. Newly developed methods can quantitatively measure the shaft base cleanliness, cross-section area, and elevated concrete temperatures during the hydration process of cast-in-place concrete foundations. Collectively, results from these tests and devices can be interpreted to evaluate the overall quality control and integrity of drilled foundations. This paper introduces three main segments of the quality control of drilled foundations: base cleanliness, drilled

3
4
5
6
7
8
9
10
11
12
13
14
15
16
17
18
19
20

Manuscript received October 18, 2017; accepted for publication March 22, 2018.

¹GRL Engineers, Inc., 30725 Aurora Rd., Solon, OH 44139, USA

²Pile Dynamics, Inc., 30725 Aurora Rd., Solon, OH 44139, USA

³ASTM Symposium on *10th International Conference on Stress Wave Theory and Testing Methods for Deep Foundations* on June 27–29, 2017 in San Diego, CA, USA.

Copyright © 2018 by ASTM International, 100 Barr Harbor Drive, PO Box C700, West Conshohocken, PA 19428-2959.

PROOF COPY [STP20170198]

224

STP 1611 On Stress Wave Theory and Testing Methods for Deep Foundations

foundation integrity, and drilled hole geometry. Primarily and for comparison purposes, for each one of the methods introduced in this manuscript, their equivalent or existing method used as the standard practice is presented and briefly discussed.

21
22
23
24**Keywords**

base cleanliness, drilled shafts, quality control, geometry, integrity

25

Introduction

In general, the specifications and guidelines for every project provide details regarding the quality control for the pertinent deep foundation system. In the particular case of drilled foundations, depending on local practice, details are provided to the interested parties regarding base cleanliness, integrity, and geometry of the drilled foundation; in some cases, all three and more testing are specified and in others selected tests are mandated. However, either way, testing is required. For example, procedures and requirements associated with shaft base cleanliness of drilled shafts designed for federally funded projects are specified in governing guidelines such as the Federal Highway Administration (FHWA) drilled shaft manual [1]. In addition, each state's department of transportation (DOT), in conjunction with the geotechnical engineer of record, provides specifications regarding allowed debris thickness limits at the shaft base [2]. In an effort to obtain the latest information regarding drilled foundation construction and quality control requirements, a large body of literature and governing documents published by each DOT were reviewed. This review process consisted of obtaining the latest version of the relevant document and identifying the section that addresses shaft base cleanliness, geometry, and integrity. From this review it was noted that the FHWA manual presents detailed guidelines regarding the quality control and quality assurance associated with drilled foundations. Therefore, it is important to present a synthesized description of the latest techniques developed for the quality control of drilled foundations.

26
27
28
29
30
31
32
33
34
35
36
37
38
39
40
41
42
43
44
45
46
47

Base Cleanliness

Several specialized inspection tools and equipment can be considered for the assessment of shaft base cleanliness as well as debris thickness determination. As a general reference, the FHWA drilled shaft manual [1] lists the tools commonly available in 2010 for quality assurance purposes, including the shaft base cleanliness. The primary tool described by the FHWA is the Miniature Shaft Inspection Device (Mini-SID), which qualitatively assesses the shaft base cleanliness based on photos and videos taken from the bottom of the drilled hole. Another inspection tool is the Shaft Quantitative Inspection Device (SQUID), which quantitatively evaluates the drilled shaft base cleanliness by measuring the debris thickness based on force and displacement measurements.

48
49
50
51
52
53
54
55
56
57
58

MINI-SID

Primarily consisting of a diving bell, the Mini-SID is equipped with a high-definition camera, light source, inlets for compressed gas and water, and three debris thickness gages located within the camera range. The test consists of locating the Mini-SID on top of the drilled hole and lowering it into the hole by using a winch (**Fig. 1**). After reaching the bottom of the drilled hole, the compressed gas will displace the fluid out of the diving bell, creating a slurry-free zone, and a photograph of the base conditions is taken (**Fig. 2**). The debris gages will indicate the approximate debris thickness. It is important to note that the outcome of this test is

59

60

61

62

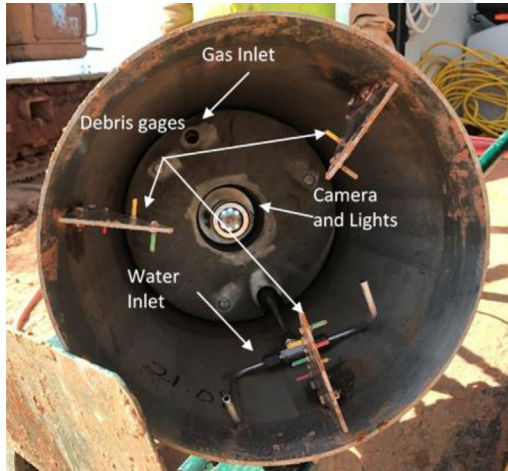
63

64

65

66

67

FIG. 1 Mini-SID: (a) diving bell and (b) preparation for testing.

(a)



(b)

PROOF COPY [STP20170198]

226

STP 1611 On Stress Wave Theory and Testing Methods for Deep Foundations

FIG. 2 Mini-SID at the bottom of a drilled shaft.

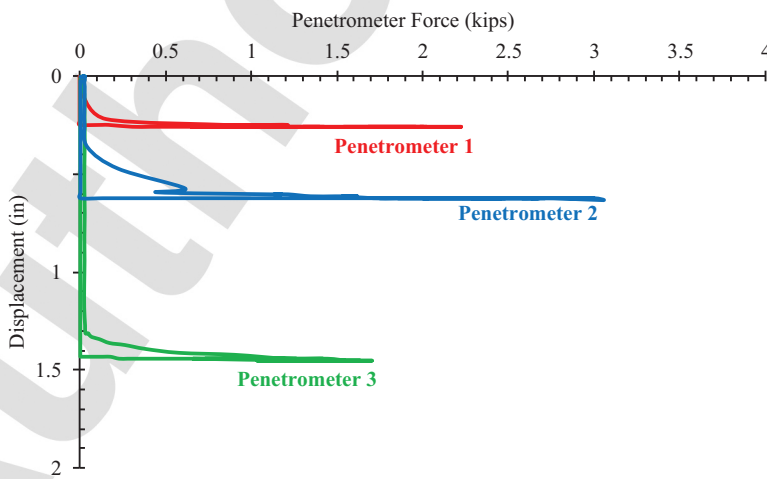
not a quantitative evaluation, and the debris thickness is marked as <0.5 or 68
>0.5 in., etc. 69

SQUID**70**

The SQUID has an octagonal shape with a maximum diagonal length of 25.5 in. 71 (647 mm) and a height of 25.0 in. (635 mm). Three penetrometers and three 72 retractable displacement plates that are used to record force and displacements 73 simultaneously are part of the device. The penetrometers are designed to have conical 74 or flat tips with an average cross-sectional area of 1.55 in.² (10 cm.²) (Fig. 3). 75 The resistance to penetration is measured by strain gages, with the capability of 76 recording up to 14 ksi (100 MPa) of stress. The test procedure consists of mounting 77 the device on the Kelly bar and lowering it into the drilled hole. Once the device is 78 located at the bottom of the hole, the buoyant weight of the Kelly bar will transfer 79 sufficient force for the probes to measure the force needed to penetrate the debris 80 and bearing layers and for the displacement plates to retract measuring the corre- 81 sponding displacements. The corresponding forces and displacements are recorded. 82 Real-time force versus displacement plots are generated and displayed in the 83 SQUID tablet (Fig. 4). 84

DEBRIS THICKNESS**85**

Based on the consistency of debris material, it is reasonably assumed that a material 86 categorized as debris will have strength properties similar to a soft-to-medium clay 87

PROOF COPY [STP20170198]**FIG. 3** SQUIDS: Shaft Quantitative Inspection Device (SQUID)**FIG. 4** Force-displacement plot from SQUID testing.

PROOF COPY [STP20170198]

228 STP 1611 On Stress Wave Theory and Testing Methods for Deep Foundations

with an unconfined compressive strength ranging from 0.25 ksf (12 kPa) to 2 ksf (95 kPa) and a unit weight ranging from 100 pcf (16 kN/m³) to 120 pcf (19 kN/m³). 88
89

With these strength parameters and applying the general bearing capacity theory 90
proposed by Terzaghi [3] for circular foundations (Eq. 1), the resistance to penetration 91
of a flat tip with a cross-section area of 1.55 in.² (10 cm²) was determined to be 92
between 0.020 kip (0.089 kN) and 0.160 kip (0.712 kN). 93

$$q_{ult} = 1.3s_u N_c \quad (1)$$

where: 94

q_{ult} = ultimate bearing capacity of a circular base, 95

s_u = undrained shear strength of the material, and 96

N_c = bearing capacity factor. 97

According to the results obtained from Eq. 1, a debris layer is defined as a material 98
that has a minimum and maximum resistance to penetrometer force of 0.020 kip 99
(0.089 kN) and 0.160 kip (0.712 kN), respectively. 100

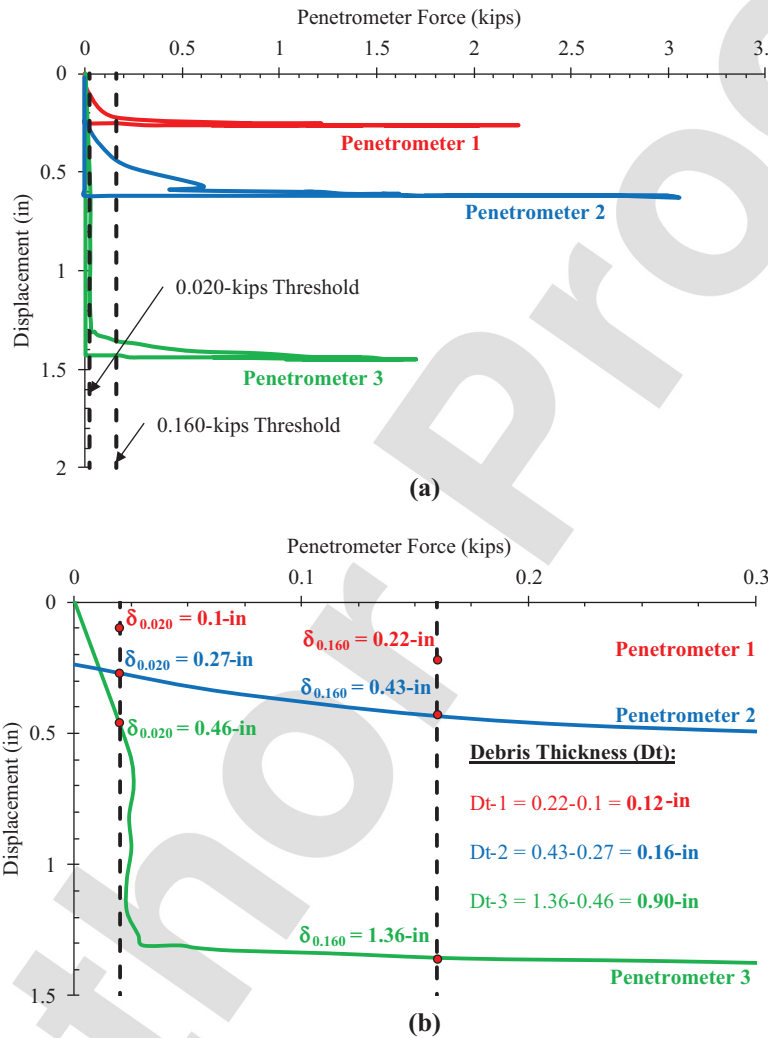
Debris thickness thresholds can be plotted on the force-displacement curves to 101
determine the debris thickness following the previously described characteristics, as 102
in Fig. 5a and b. Fig. 5a illustrates the results of a SQUID test presented as a force- 103
displacement plot that includes debris thickness thresholds. This plot includes the 104
test's loading and unloading stage, where the force and displacement gradually 105
increases to a maximum and returns to zero values as the device is unloaded. For 106
illustration purposes, Fig. 5b is an enhancement (i.e., zoom-in capture) of the 107
threshold lines, and the debris thickness is calculated by subtracting the displace- 108
ment corresponding to the soil/rock threshold (0.160 kip) from the debris threshold 109
(0.020 kip). 110

For a project located in Oklahoma, the debris thickness obtained using 111
the SQUID has been correlated to the results obtained by using the Mini-SID. 112
According to Moghaddam, Hannigan, and Anderson [4], for seven drilled shafts a 113
side-by-side base cleanliness test was performed, and the results suggest that with 114
an R^2 value of 57 % there might be a statistical correlation between debris thick- 115
nesses obtained using the Mini-SID and SQUID. 116

Drilled Foundation Integrity 117

Due to the large axial and lateral capacities, drilled shaft foundations have become 118
very popular and are widely used for federal and private projects. As previously 119
mentioned, due to the construction process associated with drilled foundations, cer- 120
tain quality control processes become very difficult to complete. During the drilling 121
process and concrete placing, some factors such as drilling cuttings, underground 122
water flow, improperly placed concrete, etc., could significantly affect foundation 123
quality. Several non-destructive testing (NDT) methods are available for evaluating 124
the integrity of completed drilled shafts which are briefly described and discussed 125
herein. 126

FIG. 5 Debris thickness from SQUID testing: (a) overall thresholds and (b) debris thickness calculation.



THERMAL INTEGRITY PROFILING

127

Thermal integrity profiling (TIP) is an NDT method that uses the heat generated by hydrating concrete to determine the integrity of the drilled shaft. These temperature measurements are obtained throughout the shaft length using thermal sensors [5–7]. Additional information such as reinforcing cage eccentricities and concrete cover can be obtained from the TIP analysis. Furthermore, this method allows for the detection of defects within the rebar cage as well as in the cover area. 128
129
130
131
132
133

PROOF COPY [STP20170198]

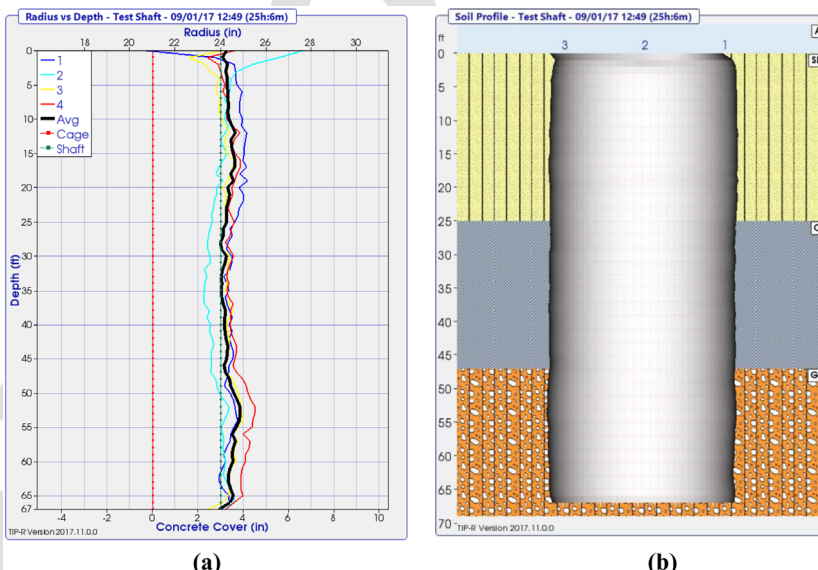
230 STP 1611 On Stress Wave Theory and Testing Methods for Deep Foundations

For example, if a series of drilled shafts are used for a retaining wall project (i.e., secant or tangent walls), the cover and verification of concrete flowing around and through the cage to provide pertinent cover becomes important. Local temperatures are converted to local radii based on temperature measurements at various locations along the drilled shaft or augered-cast pile as well as the total concrete volume (Fig. 6).

Curing concrete will exhibit a normal heat signature that is dependent upon the shaft diameter, concrete mix design, concrete quality, and soil conditions. A local reduction in cement content within the concrete will interrupt the normal temperature signature and will be measured by the TIP as a locally reduced temperature in the area of the defect compared with the overall average temperature. This defect will also be seen in adjacent measurement locations, with a diminished effect at more distant measurement locations. Any temperature measurements that are cooler than the average temperature are areas of reduced cement content that can be a reduction in concrete volume (i.e., defect) or poor concrete quality. Temperature measurements with a higher local temperature than the average temperature are areas of increased concrete volume (i.e., bulge).

The TIP test can also evaluate the reinforcing cage alignment by comparing temperature measurements from diametrically opposite locations versus the overall average temperature at the same elevation. If one temperature measurement

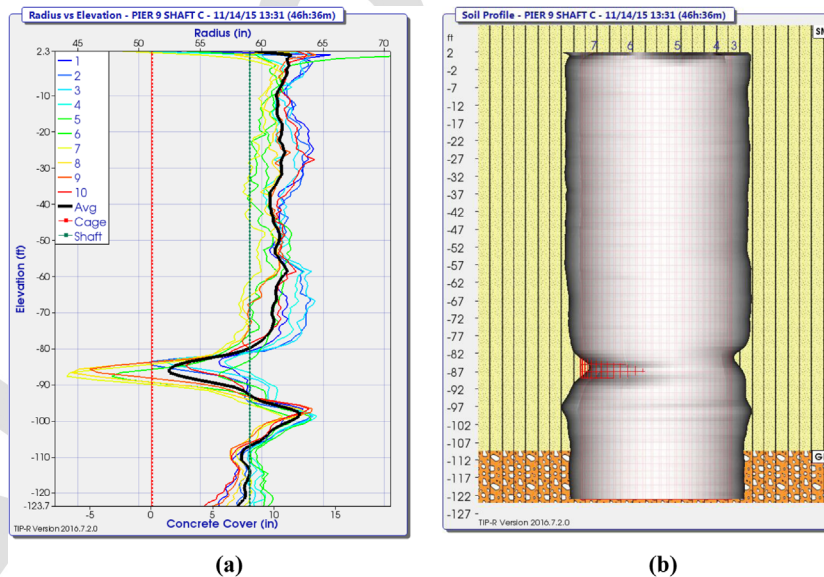
FIG. 6 Thermal integrity profiling results for a satisfactory drilled shaft: (a) effective radius versus depth and (b) three-dimensional model overlaying the soil profile.



PROOF COPY [STP20170198]

location is cooler than the average temperature and the diametrically opposite temperature measurement location is warmer than the average temperature, this indicates that the cage is not centered. The cooler measurements indicate this area of the reinforcing cage is shifted toward the soil interface, whereas the warmer measurements indicate this area of the reinforcing cage is shifted toward the shaft center. This cage alignment analysis provides additional information on concrete cover because a reinforcing cage that is shifted to the excavation sidewall can result in little or no concrete cover in this region, even without having a defect present. These effects and analyses are further illustrated by Fig. 7, in which the effective average radius (inches) versus elevation (feet) (Fig. 7a) and the three-dimensional image of the drilled shaft (Fig. 7b) are created based on the reported concrete volume and reported cage radius. The effective average radius is the computed average radius at a given depth based on the average of all recorded local temperatures. The vertical dashed green line represents the design or intended shaft diameter, the vertical dashed red line represents the edge of the reinforcing cage, and the estimated cover beyond the reinforcing cage is shown along the x axis. Note that from the top of the shaft to elevation (EL)-78, the effective average radius is slightly greater than the design shaft radius of 59 in. This slightly oversized region is consistent with the reported concrete over pour. Beginning at EL-78, the effective average

FIG. 7 Thermal integrity profiling wire results for a defective drilled shaft: (a) effective radius versus elevation and (b) three-dimensional model overlaying the soil profile.



PROOF COPY [STP20170198]

232 STP 1611 On Stress Wave Theory and Testing Methods for Deep Foundations

radius is reduced to 52 in. near EL-85.70. The effective local radii are reduced to 173 approximately 44 to 45 in. near Wire 7 and Wire 8. An increase in cover or excess 174 concrete is evidenced by higher recorded temperatures near EL-98. The effective 175 average radius is relatively consistent with the design radius from EL-106 to the 176 base of the shaft. 177

Due to the estimated reduction in the radius to inside the reinforcing cage 178 shown in Fig. 7, the drilled shaft was cored to try to locate the extent of the anomaly 179 (Fig. 8). Because coring outside the cage is in most cases not feasible, the first core 180 was reportedly drilled 18 in. inside the reinforcing cage between Wire 7 and Wire 8. 181 This location was selected because Wire 7 and Wire 8 showed the maximum reduc- 182 tion in the radius. The core was angled slightly so that near EL-87 the core would 183 be in close proximity to the cage. As shown in Fig. 8, the results of coring showed 184 the poor quality of concrete that could have been missed if the coring would have 185 been done through the center. 186

Drilled Foundation Geometry

187

Drilled shafts are being increasingly used as a deep foundation element due to their 188 ability to carry large loads. These shafts are difficult to inspect prior to the concrete 189 casting process, particularly when they are drilled under wet conditions. The exca- 190 vation shape, cross-sectional area, and verticality are being inspected using various 191 techniques to verify design compliance. Depending on the foundation diameter, the 192 verticality plays an important role during the load-transfer process, and in cases in 193 which the foundation is rock-socketed, the verticality could significantly affect the 194

FIG. 8 Coring results in a defective drilled shaft.



foundation performance under eccentric loads at the transition zone between soil 195 and rock. 196

The various inspection techniques used include concrete volume plots determined using a weighted tape, mechanical calipers using spring-loaded arms, and electronic calipers using ultrasonic signals. The advantages and limitations of each of these methods, along with a new inspection device, are presented in the sections 197 198 199 200 201 that follow.

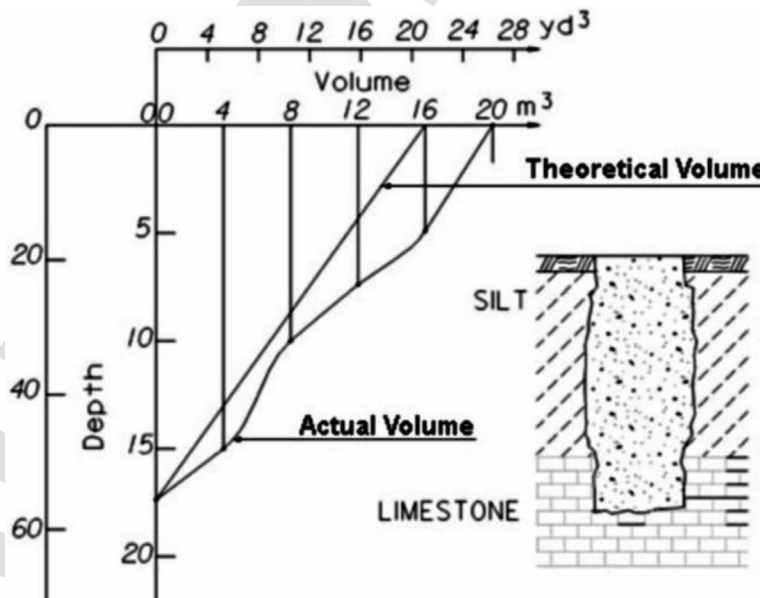
CONCRETE VOLUME PLOTS

The most basic method for determining the excavation shape is the use of manually 203 created concrete plots (**Fig. 9**). This method determines the shape of the excavation 204 by using a weighted tape to measure the top of the concrete elevation relative to the 205 placed concrete volume. This test method provides a crude estimation of the excava- 206 tion shape because it relies completely on the skill level of the individual taking 207 measurements with the weighted tape and further relies on the reported truck vol- 208 umes from the ready-mix plant, making the method subjective with no quantitative 209 measurements. 210

THE MECHANICAL CALIPER

The drilled hole shape could also be assessed using a mechanical caliper, which 212 relies upon a device consisting of two or four spring-loaded arms that contact the 213

FIG. 9 Concrete volume-depth plot for assessing drilled hole shape.



PROOF COPY [STP20170198]

234 STP 1611 On Stress Wave Theory and Testing Methods for Deep Foundations

excavation sidewalls as the device is lowered or raised through the excavation (Fig. 10). The arm movement is measured electronically to determine the distance from the center to the sidewall at the various measurement points. The mechanical devices must be advanced slowly to ensure the arms remain in contact with the sidewall and do not slip during advancement. The mechanical caliper provides a minimal amount of quantitative data (geometry determined from data taken on either a 90 or 180° axis) depending upon the number of spring-loaded arms and relies upon these arms staying in contact with the sidewalls during the entire lowering/raising process.

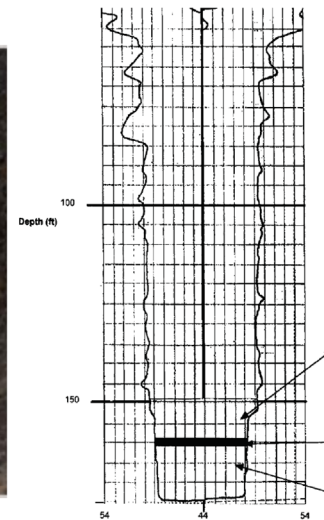
SONAR CALIPER

The electronic caliper method involves transmitting an ultrasonic pulse through a wet-cast excavation and receiving the pulse that has reflected off the excavation sidewall. The distance to the sidewall is calculated from one-half the measured transmit/receive pulse time multiplied by the wave speed of the slurry material [8,9] (Fig. 11). Some electronic calipers have two or four ultrasonic sensors mounted in fixed positions and thus provide a minimal amount of quantitative data (geometry determined from data taken on either a 90 or 180° axis). Other electronic calipers are rotated 360° at discrete elevations to obtain these transmission times, providing a greatly increased number of data measurements at each measurement elevation. The caliper depth within the slurry is measured via a depth encoder located at the surface, tracking a cable connected to the electronic caliper. The distance to each

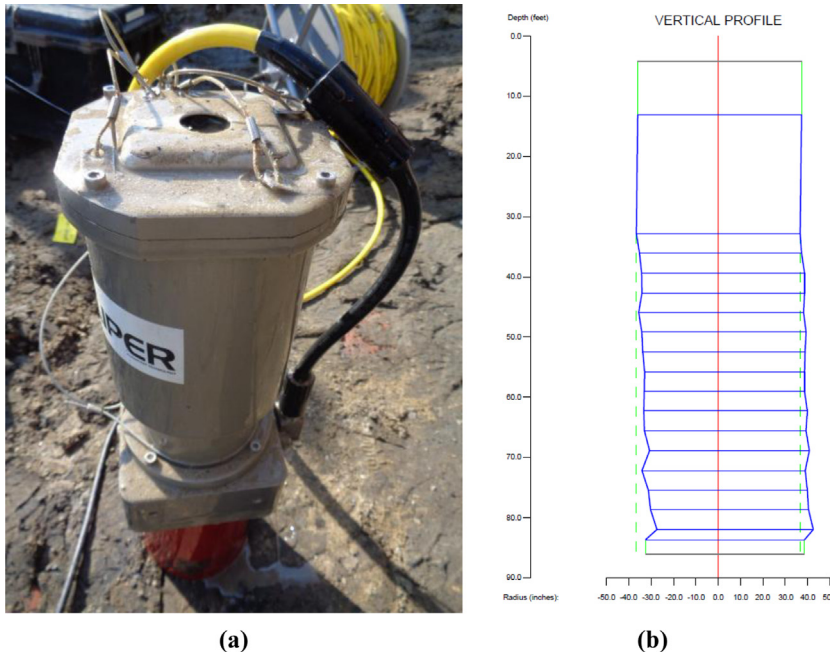
FIG. 10 Mechanical caliper (a) during testing and (b) testing results.



(a)



(b)

FIG. 11 Sonar caliper (a) before testing and (b) testing results.

sidewall is calculated using an assumed wave speed or a wave speed that is measured only near the surface. As soil particles segregate within the slurry, these particles naturally sink to the bottom of the excavation, increasing the slurry density and changing the wave speed with depth. These changing slurry properties as a function of depth, and thus a changing wave speed as a function of depth, can cause significant errors in the shape or cross-section calculation.

SHAFT AREA PROFILE EVALUATOR

241

The Shaft Area Profile Evaluator (SHAPE) device attaches to the Kelly-bar stub and collects data while advancing down the excavation at comparatively high rates of speed (~305-mm/s [1-ft/s] advancement rate). This advancement rate greatly reduces the time required to profile the shaft sidewalls. The device simultaneously transmits and receives ultrasonic signals from eight individual sensors mounted 45° apart, providing the needed resolution to more accurately determine the excavation geometry (Fig. 12). If additional resolution is required, the device can complete the downward scan, and then the Kelly bar can be rotated the appropriate degree with additional data taken at each depth location while the device is raised to the surface.

242

243

244

245

246

247

248

249

250

To overcome the variability in slurry wave speed, the SHAPE has an integrated self-calibrating feature that measures the transmission time through the slurry at

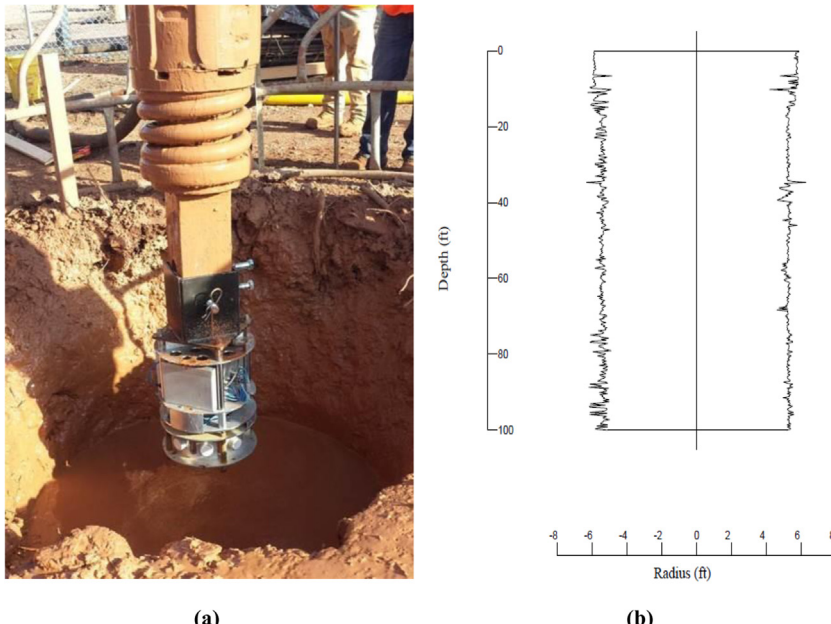
251

252

PROOF COPY [STP20170198]

236

STP 1611 On Stress Wave Theory and Testing Methods for Deep Foundations

FIG. 12 SHAPE (a) before testing and (b) testing results.

(a)

(b)

each depth measurement location utilizing a transmitter and receiver pair that are 253 mounted a known distance apart. Each radii calculation is performed using the 254 actual measured wave speed at its respective depth, thus improving the accuracy of 255 the computed radii and overall verticality of the excavation. The device operates 256 with no electronic cables needed for data transmission from the device to the 257 surface, thereby keeping personnel away from the open excavation during the test. 258 When the device is raised to the surface, the measured data are transmitted to a 259 tablet computer located a safe distance from the excavation for further evaluation. 260

The eight sensors and frequency of the transmitted and received signals allow 261 the device to acquire a highly quantitative excavation shape while allowing the 262 device to be lowered at a high and constant rate on the drilling stem, with no stop- 263 ping required at each measurement location as other devices require. 264

Summary and Conclusions

265

Considering the primary objective of testing drilled foundations combined with 266 the impact of time effectiveness on construction project schedules, the new imple- 267 mented methods for testing the base cleanliness, integrity, and geometry of drilled 268 foundations could benefit the construction quality and schedule by providing reli- 269 able and efficient results. The ability of quantitatively assessing the quality of the 270

drilled foundations provides a better basis for the overall evaluation of deep foundations. It is important to reiterate that a properly documented construction process, including quality control of materials, quality control of the drilling process, and inspection of the drilled hole prior to placing concrete, leads to a high-quality foundation construction. Therefore, equipment and methods that help to achieve this objective always benefit the industry, but only if the process is completed safely, validly, and efficiently.

References

278

- [1] Al Hai, and Al Mukaddam, "Mechanical Caliper Logging (MCL)," <https://web.archive.org/web/20170228004004/http://www.ahamgeo.com/mechanical.html> (accessed 14 Mar. 2018). 279
280
281
- [2] Brown, D. A., Turner, J. P., and Castelli, R. J., *Drilled Shafts: Construction Procedures and LRFD Design Methods*, U.S. Department of Transportation, Federal Highway Administration, Washington, DC, 2010. 282
283
284
- [3] Terzaghi, K., *Theoretical Soil Mechanics*, Wiley, New York, 1944. 285
- [4] Moghaddam, R. B., Hannigan, P. J., and Anderson, K., "Quantitative Assessment of Drilled Shafts Base-Cleanliness Using the Shaft Quantitative Inspection Device (SQUID)," *IFCEE 2018: Recent Developments in Geotechnical Engineering Practice*, A. Lemnitzer, A. W. Stuedlein, and M. T. Suleiman, Eds., American Society of Civil Engineers, Reston, VA, 2018. pp. 575-588 286
287
288
289
290
- [5] Mullins, G. and Winters, D., *Infrared Thermal Integrity Testing Quality Assurance Test Method to Detect Drilled Shaft Defects*, Final Report, No. WA-RD 770.1, Washington State Department of Transportation, Olympia, WA, 2011. 291
292
293
- [6] Mullins, G. and Ashmawy, A. K., *Factors Affecting Anomaly Formation in Drilled Shafts*, Final Report, University of South Florida, Tampa, FL, 2005. 294
295
- [7] Mullins, G. and Kranc, S. C., *Thermal Integrity Testing of Drilled Shaft*, Final Report, University of South Florida, Tampa, FL, 2007. 296
297
- [8] Matrix Construction Products. <http://www.matrixcp.com> (accessed March 14, 2018). 298
- [9] Seo, H., Moghaddam, R. B., Surles, J. G., and Lawson, W. D., *Implementation of LRFD Geotechnical Design for Deep Foundations Using Texas Cone Penetrometer (TCP) Test*, No. FHWA/TX-16/5-6788-01-1, Texas Tech University, Lubbock, TX, 2016. 299
300
301